Journal of Theoretical and Applied Information Technology
28th February 2026. Vol.104. No.4

ISSN: 1992-8645 www.jatit.org E-ISSN: 1817-3195

HYBRID DEEP LEARNING AND OPTIMIZATION-DRIVEN FRAMEWORK FOR ENHANCED SKIN CANCER DETECTION AND CLASSIFICATION

A CHANDRA SEKHAR [1] , D VENKATESH [2]

[1]Research Scholar, Department of Computer Science and Engineering, Jawaharlal Nehru Technological University, Anantapur, Andhra Pradesh, India

[2]Professor, Department of Computer Science and Engineering, PVKK Institute of Technology, Anantapur, Andhra Pradesh, India

E-mail: [1]chandra.ambarapu@gmail.com, [2]deancseit@gmail.com

ABSTRACT

Globally, skin cancer is one of the most common diseases caused by excessive exposure to ultraviolet (UV) radiation. The outcomes and prognosis for treating skin malignancies significantly improve with early detection and accurate diagnosis. However, many diagnostic methods have limitations, entail high computational costs, rely heavily on manual feature extraction, lack good generalization across datasets, and are susceptible to adversarial attacks. This paper addresses these limitations in skin cancer diagnosis by proposing an improved Wavelet-AHE Diffusion Enhanced Hybrid Network (WADE-HNet) for enhancing detection as well as classification. The proposed ensemble technique integrates ResEff-FuseNet for feature extraction, Firefly-Bitterling Adaptive Selection Optimization (FBASO) for optimal feature selection, Multi-Stage Attention Capsule Network (MSA-CapsNet) for enhanced classification performance, and Modified U-Net++ for lesion segmentation. Such improvements increase the interpretability, generalizability, and computational efficiency of model performance. Finally, empirical results for both the HAM10000 and ISIC 2019 datasets validate that WADE-HNet outperforms benchmark models with a high accuracy of 99.39%. In this way, the proposed strategy ensures consistency in clinical usage while reducing false positives and false negatives.

Keywords: *Skin Cancer Detection, DL, Feature Selection, Capsule Networks, Optimization, Image Processing, WADE-HNet*

1. INTRODUCTION

Skin cancer, one of the most prevalent cancers globally, is primarily caused by prolonged exposure to ultraviolet (UV) radiation. Early detection of skin cancer is crucial, as it significantly enhances the chances of successful treatment and survival. However, despite significant advancements in diagnostic techniques, such as histology and dermoscopy, these methods are time-consuming, require high expertise, and often suffer from limitations such as high computational costs and dependency on manual feature extraction. Moreover, these methods struggle to generalize across diverse datasets, and the reliance on expert knowledge makes them ineffective for more complex lesion patterns.

In recent years, skin cancer detection has gained significant attention in the medical imaging and artificial intelligence (AI) communities. Numerous methods have been proposed to automate the diagnosis of skin lesions, primarily using deep learning (DL) techniques. Traditional machine learning (ML) models, such as Support Vector Machines (SVMs) and decision trees, have been employed, but these approaches often struggle with the complexities of skin lesion images and require extensive manual feature engineering. In contrast, DL models, particularly Convolutional Neural Networks (CNNs), have shown promise in directly learning hierarchical features from raw image data, eliminating the need for manual feature extraction [1,2].

In today's scenario, one of the most prevalent types of cancer in the modern world is skin cancer, which is typically brought on by prolonged exposure to UV light. Early detection of skin cancer improves the likelihood of receiving treatment and surviving it [2]. Modern diagnostic techniques involve histology, dermoscopy, and inspection [3–4] which require a great deal of time as well as a high level of expertise. CAD systems aim to assist dermatologists in identifying malignant tumors with precision. However, their effectiveness depends on accurately identifying and classifying the pertinent features [5].

Previously, melanoma diagnosis has often employed traditional methods like rule-based image analysis, manually derived feature extraction, and machine learning (ML) based classification [6]. These approaches often perform poorly on a variety of datasets and mostly deal with manually chosen color, texture, and shape descriptors [7]. Additionally, the light condition and skin types, taking into account all lesion appearances, may lead to incorrect categorization [8]. The majority of these methods have also been criticized for relying on expert knowledge to select features, which makes them ineffectual for complicated patterns because they need the addition of additional features [9]. These methods' overall dependability for clinical applications is lowered as a result of their high false-positive and false-negative rates [10].

Using CNNs to directly learn hierarchical visual properties from raw images, DL has quickly become a potent method for autonomous skin cancer diagnosis [11]. DL does what previous methods couldn't. Because these models can recognize subtle patterns in the training data, they are less reliant on human feature engineering for accurate classification [12]. Some of the most recent cutting-edge DL models, including ResNet, VGG, and EfficientNet, have demonstrated exceptional performance in the diagnosis of skin cancer and melanoma [13]. Unfortunately, DL is computationally costly to process, relies on big annotated data sets in order to have optimal results, and was recently found to be susceptible to adversarial attacks [14]. In addition, the physician is generally not able to comprehend the reasoning process since these models are often black boxes [15]. CNNs and DL approaches were introduced by Ali et al. in 2021 [16] to categorise skin lesions as either benign or malignant. AlexNet, ResNet, and VGG-16 were examples of transfer learning (TL) models that greatly enhanced the classification of skin lesions. Model performance is improved through data preparation techniques such as augmentation, normalization, and reduction of noise. A unique deep CNN was trained using the Adam optimizer and cross-entropy loss on the HAM10000 dataset. Measures such as accuracy, precision, recall, and F1 score are used to assess the model's performance in comparison to TL techniques.

In 2022, Anand et al. [17] looked into DL and TL techniques including VGG16, ResNet, and AlexNet that have been used in skin cancer classification studies. They all turned out to have pretty accurate conclusions. To improve the model's performance, the dataset has been pre-processed using methods such as data augmentation, normalization, and noise reduction. In 2020, Monika et al [18] proposed ML and image processing techniques that have been suggested for dermoscopic analysis and classification of skin cancers. The preprocessing techniques by which lesions can be made more distinguishable include hair removal, picture noise reduction, and image smoothing. Shaikh et al. [19] showed in 2022 that CNNs can compete with dermatologists in the multiclass categorization of skin cancer, especially when they use TL and pre-trained ImageNet weights. In 2022, Fraiwan, M & Faouri [20] proposed deep TL for skin lesions that can be classified with high accuracy and without the need for explicit feature extraction. Several studies in the field have classified dermoscopic images using a variety of pre-trained models, demonstrating how sample distribution and imbalance within a dataset impact performance. Shorfuzzaman [21] presented ensemble DL techniques for melanoma classification in 2022 with the aim of enhancing classification precision with TL. To demonstrate how a meta-learner enhances the predictions made by several CNN models that were accomplishing the same task, they employed stacking frameworks. Employing interpretability strategies, such as heatmaps, enhanced the clinical usability of the models. In 2020, Jinnai et al [22] demonstrated that DL models that are capable of classifying skin kinds of lesions are more accurate than dermatologists in both binary and multiclass classifications. A total of 5846 clinical photos were gathered from 3551 patients; 4732 of these images were utilized for training with bounding-box annotations, and 666 patients were included for testing. After evaluation and training, the Faster R-CNN (FRCNN) model outperformed 20 dermatologists in terms of diagnosis, with 86.2% classification accuracy across six categories and 91.5% accuracy across two. Gouda et al. [23] proposed employing CNN-based TL models along with other DL techniques for high-precision skin lesion classification in 2022. Inception-ResNet achieved accuracy values of 83.7%, 85.8%, and 84%, respectively.

In 2020, Nahata & Singh [24] introduced DL methods to improve precision, and CNNs have become a viable choice for classifying skin cancer. In 2022, Mehr & Ameri [25] demonstrated that DL techniques could be utilized to distinguish between healthy skin and skin cancer, as well as to enhance

stereoscopic and diagnostic accuracy by adding patient metadata to the lesion image. To enhance models in the unique categorization of lesion images, construct Inception-ResNet-v2 networks employing TL.

From the above study, it is clear that in [16] requires extensive preprocessing, in [17] limited dataset impacts generalizability, in [18] relies on handcrafted feature extraction, in [19] high-class imbalance affects classification, in [20] dataset imbalance affected performance, in [21] model complexity increases computational cost, in [22] requires large annotated datasets, in [23] requires extensive preprocessing, in [24] computationally expensive, in [25] requires additional patient data for training. Hence, there is a need for novelty to overcome these challenges.

The main objective of this study is to develop a hybrid framework that can handle the challenges of data imbalance, high computational costs, and poor generalization, while providing accurate and interpretable results for clinical applications. This approach promises to not only improve diagnostic accuracy but also reduce computational overhead, making it more suitable for real-time implementation in clinical environments.

Research Problem: We highlight the limitations of existing skin cancer detection methods, including high computational costs, reliance on manual feature extraction, and poor generalization across datasets.

Research Objectives: The goal is to propose the WADE-HNet framework to enhance accuracy, efficiency, and robustness in skin cancer detection by integrating various state-of-the-art models and techniques.

Significance: Our approach offers improved accuracy, reduced false positives/negatives, and better computational efficiency, with potential for clinical application to enhance patient outcomes.

Research Gap: The study fills the gap by combining deep learning with optimization techniques to overcome issues such as dataset imbalance, high computational cost, and lack of interpretability.

The hybrid nature of WADE-HNet ensures better generalization across diverse datasets, reduces computational overhead, and enhances interpretability, making it a promising solution for clinical deployment in skin cancer detection.

2. PROPOSED METHODOLOGY

Skin cancer is currently one of the most common cancers. It occurs when prolonged exposure to UV light causes skin cells to proliferate excessively. Finding skin cancer early boosts the chances of successful treatment and survival. This study aims to spot skin cancer with precision. Yet, current skin cancer detection models run into several problems. These include needing lots of prep work, dealing with uneven datasets and high computing costs, depending on hand-made features limited to use across different cases, and requiring large labeled datasets or extra patient info. All these issues affect how well they diagnose the disease. To overcome these issues, a novel Wavelet-AHE Diffusion Enhanced Hybrid Network (WADE-HNet) is introduced in this approach, ensuring higher accuracy, robustness, and efficiency in medical diagnosis. Figure 1 shows the proposed WADE-HNet architecture for improved skin cancer detection.

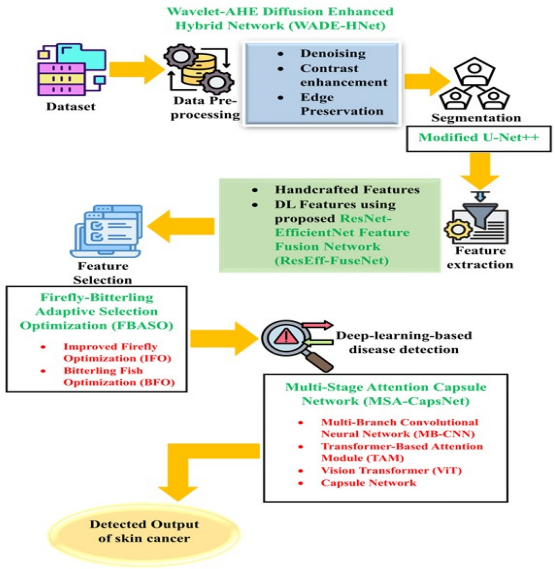

Figure 1: Architecture of the proposed WADE-HNet model

2.1 Data Collection

Both benign and cancerous skin mole images are divided equally in this sample. The information has been separated into two folders that each contain 1800 images of size 224x244 of the two-mole species.

2.2 Data Pre-processing

Preprocessing is the process of applying several methods to skin lesion images to increase the detection rate. These techniques include image enhancement to improve contrast, noise reduction to eliminate artifacts, lesion segmentation, normalization to make the lesion consistent, data

augmentation to enable the further generalization of the model, and colour space conversion to enhance a lesion's features, maintaining the most accurate input for feature extraction and classification.

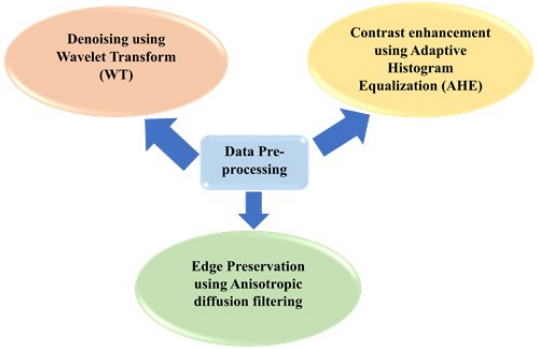

Figure 2: Data Pre-processing

extraction and classification

2.3 Denoising

One preprocessing method for removing image noise while keeping the key elements is called denoising. By separating an image into its approximation and detail coefficients, wavelet transform-based denoising allows for the selective thresholding of high-frequency noise in enhanced skin cancer detection and classification. This makes the image clearer, which helps with precise feature extraction and categorization.

2.4 Wavelet Transform (WT)

In the process of detecting and classifying skin cancer, we increase the visibility of the lesions by employing a power example DWT application to suppress distracting artefacts while maintaining crucial structural details. The initial image represents $I(x,y)$, the approximation coefficient represents $C_A(m,n)$, and the horizontal, vertical, and diagonal detail coefficients represent $C_d(m,n)(for\ d \in H,V,D)$ in equation (1) The scaling function represents $\varphi_{m,n}$, and the wavelet basis function is $\psi^d_{m,n}$.

$$I(x,y) = \sum_{m,n} C_A(m,n)\varphi_{m,n}(x,y) + \sum_{m,n}\sum_{d\in\{H,V,D\}} c_d(m,n)\psi^d_{m,n}(x,y) \quad (1)$$

Common spatial famelet frames C_H, C_V, C_D were subjected to hard or soft thresholding to reduce noise and preserve edge features.

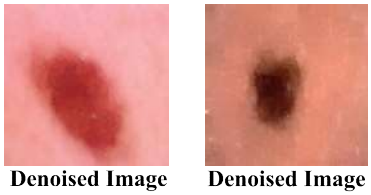

Denoised Image of Benign **Denoised Image of Malignant**

Figure 3: Image results of denoising for the Benign and Malignant

Contrast enhancement improves the visibility of details by adjusting the intensity distributions of images, thereby making certain characteristics more pronounced. This improvement improves the definition of certain key traits. By using Adaptive Histogram Equalization (AHE) approaches to improve the contrast of the lesions, this work aims to improve analysis and classification.

AHE is a technique for improving image contrast that, unlike histogram equalization, redistributes the pixel intensity at specific small areas within the image. This makes use of small local regions for the computation of the CDF that foreground features in low-contrast areas. Thus, AHE helps to depict lesion shapes in Enhanced Skin Cancer Detection and Classification, which enhances feature extraction and classification skills.

Pseudocode for Feature Extraction:

```
def feature_extraction(image):
  # Preprocess image
  preprocessed_image = preprocess(image)
    # Feature extraction using ResEff-FuseNet
  resnet_features = ResNet50(preprocessed_image)
  efficientnet_features = EfficientNet(preprocessed_image)
    # Fuse the extracted features
  fused_features = concatenate(resnet_features, efficientnet_features)
    return fused_features
```

Based on equation (2-4), the intensity probability distribution function (PDF) is given here as I(x,y), the number of pixels of intensity I is given by n_I, the total number of pixels in the region is given by N, and the maximum intensity is given by L:

$P(I)=n_I/N$ (2)

C(I)=∑_(j=0)^Ip(j) (3)

I^' (x, y)=C(I(x, y)×(L-1) (4)

Following data segmentation, the resultant data is fed into the feature extraction procedure. Feature extraction is the process of identifying and measuring important elements like texture, shape, color, and edge patterns, and it is utilized to distinguish between malignant and euthanized lesions. Some of the image preprocessing techniques and methods for obtaining descriptors include color histograms, deep-learning feature maps, and wavelet-based texture analysis. By presenting the different machine-learning or deep-learning algorithms with the most discriminative

information, precise feature extraction enhances classification precision. Figure 4 illustrates the feature extraction process. The pixel intensity distribution across several color spaces (RGB, HSV, and CIE) is represented by the artificial color presentation characteristics. Skin lesions are described using less than that. The color histogram and its statistical measures support in the better detection and classification of skin cancer by separating malignant and benign lesions through their pigmentation patterns.

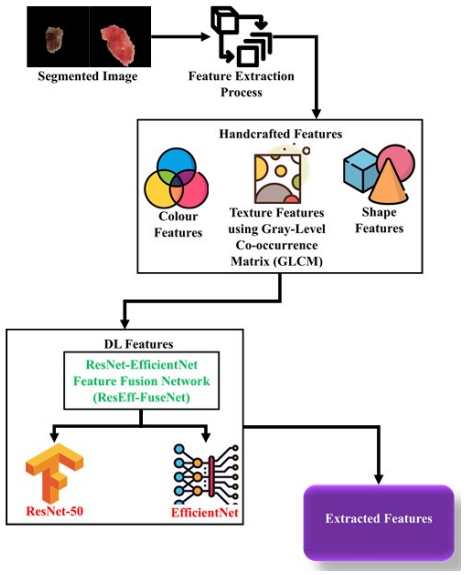

Figure 4: Process of feature extraction

2.5 ResNet-50 + EfficientNet Hybrid Model

EfficientNet's efficient scaling method and ResNet-50's deep residual learning capabilities are used to create a hybridized model, ResEff-FuseNet, that extracts both matching high-level characteristics and fine-grained features of a lesion. Through improved texture, form, and structural pattern capture, this approach improves feature representation. Equation (15), in which [.] refers to concatenation, takes advantage of the capabilities of both architectures to enhance the classification precision in Enhanced Skin Cancer Detection and Classification.

$$F_{hybrid} - [F_{ResNet}, F_{EfficientNet}] \quad (5)$$

This increases the diagnosis and identification accuracy of skin cancer by ResEff-FuseNet features with individually produced, fine-tuned features (color, texture, and form). While DL features recognize intricate patterns to provide reliable and thorough diagnostic systems, handcrafted features offer interpretable domain knowledge.

2.6 Initial Feature Reduction using Improved Firefly Optimization (IFO)

IFO is employed as the first-stage feature selection approach to eliminate noisy features and enhance search efficiency. The algorithm starts by initializing the fireflies using random subsets of features from *F*. Each firefly is a candidate feature subset, and the brightness of a firefly is calculated based on the fitness function, which is calculated using the classification accuracy based on a base classifier (e.g., SVM, Random Forest). Fireflies approach more naturally looking (brighter) solutions through the attractiveness function as per the equation

$$x_i^{t+1} = x_i^t \mid \beta e^{-\gamma r^2}\left(x_j^t \quad x_i^t\right) \mid \alpha\epsilon_i \quad (6)$$

Where, β is the attraction parameter, γ determines the light absorption, α is the randomization parameter, ϵ_i is a randomly chosen number drawn from a Gaussian distribution, and x_i^t is the position of Firefly i at iteration t.

The process is repeated iteratively until convergence conditions are fulfilled, i.e., minimal redundancy among the features and enhanced classification accuracy. The resultant feature subset is the top m highest-fitness features, which are preserved for subsequent refinement.

2.7Refinement using Bitterling Fish Optimization (BFO)

Then, BFO strikes a balance between exploitation and exploration in search of local optima to maximize the selected features chosen by IFO. A fish population is initialized at algorithm onset, with each fish being a candidate feature subset picked from IFO. Every fish computes its fitness in terms of feature importance and classification accuracy. While swimming in a swarm, fish align their positions based on personal experience and shared knowledge according to the following equation (7):

$$X_i^{t+1} = X_i^t + w_1\left(X_g - X_i^t\right) + w_2(X_b - X_i^t) + \eta\delta \quad (7)$$

Where X_i^t is the position of the fish in iteration t, X_g is the global best solution, X_b is the local best solution in the neighborhood of the fish, w_1 and w_2 are the weighting factors, η is a randomization factor, and δ is a Gaussian-distributed noise. The fitness of each fish is calculated through a weighted sum of classification accuracy and feature importance as per the equation (8):

$$F_i = \lambda_1 \times \text{Accuracy} + \lambda_2 \times \text{FeatureImportance} \quad (8)$$

Where, F_i denotes the fitness score of fish i, λ_1 and λ_2 are weighting parameters trading accuracy and feature importance. The algorithm repeatedly improves the feature subset by eliminating redundant and less informative features. The convergence is achieved when no improvement in classification accuracy is found. The final optimal feature subset is selected based on the highest-ranked solutions as per the equation (9):

$$S_{final} = \{f_i | F_i \geq \theta\} \quad (9)$$

Where, S_{final} is the last selected feature subset, θ is a predetermined threshold such that only the most useful features are preserved.

Pseudocode for FBASO

```
def FBASO(features):
    # Initialize fireflies with random feature subsets
    fireflies = initialize_fireflies(features)

    # Evaluate fitness of each firefly
    for firefly in fireflies:
        fitness = evaluate_fitness(firefly)

    # Update positions and select optimal features
    optimal_features = select_optimal_features(fireflies)

    return optimal_features
```

Pseudocode for MSA-CapsNet:

```
def MSA_CapsNet(features):
    # Apply multi-branch convolutions
    convolutional_features = multi_branch_convolutions(features)

    # Apply attention mechanisms
    attention_features = apply_attention(convolutional_features)

    # Classification using capsule networks
    predictions = capsule_network(attention_features)

    return predictions
```

FBASO improves classification accuracy by choosing the most discriminative features and minimizing computational complexity. This approach improves skin cancer classification's accuracy and efficiency, making it more suitable for practical uses.

3.RESULTS AND DISCUSSION

This section discusses the experimental setup findings of the proposed hybrid DL and optimization-driven skin cancer diagnosis framework based on classification accuracy, segmentation, and feature selection. The comparison with other existing models gives a significant insight that the proposed approach is capable of improving diagnostic accuracy, with a reduction in computational complexity.

3.1 Research Method and Execution Protocol

To evaluate the proposed WADE-HNet framework for skin cancer detection, a detailed experimental setup was designed. This section outlines the dataset description, data preprocessing steps, algorithm parameter settings, and the hardware and software environment used during the experiments.

Dataset Description:

We used two publicly available datasets to evaluate the performance of the proposed framework:

HAM10000 Dataset: This dataset contains 10,000 dermoscopic images representing a variety of skin lesions. The dataset includes both malignant (melanoma) and benign (non-melanoma) lesions, providing a balanced dataset for training and testing.

ISIC 2019 Dataset: The International Skin Imaging Collaboration (ISIC) 2019 dataset contains 25,000 dermoscopic images of skin lesions, including melanoma and other non-melanoma categories. This dataset is widely used in skin cancer detection research.

For both datasets, the images were split into training and testing sets, with 80% of the data used for training and 20% reserved for testing.

Data Preprocessing Steps:

The following preprocessing steps were applied to the datasets before feeding them into the WADE-HNet model:

Image Enhancement: Adaptive Histogram Equalization (AHE) was applied to improve the contrast of the images, making the lesions more visible.

Noise Reduction: Wavelet Transform (WT)-based denoising was used to remove high-frequency noise while preserving critical lesion features.

Segmentation: Lesions were segmented using the Modified U-Net++ model, which utilized dense skip connections and multi-scale fusion to isolate the regions of interest for classification.

Parameter Settings for Algorithms:

For training the models, the following parameter settings were used:

ResEff-FuseNet:

Learning rate: 0.001
Batch size: 32
Epochs: 50

FBASO (Firefly-Bitterling Adaptive Selection Optimization):

Population size: 50
Maximum iterations: 100
Convergence threshold: 0.001
MSA-CapsNet:
Capsule size: 16
Number of capsules: 5
Learning rate: 0.0005
Batch size: 16
Epochs: 50

The experiments were conducted on the following hardware and software setup:

- **Hardware**:
  - CPU: Intel i7-10700K @ 3.80 GHz (8 cores, 16 threads)
  - GPU: NVIDIA GeForce RTX 3080 (10 GB)
  - RAM: 32 GB
- **Software**:
  - Programming Language: Python 3.8
  - Frameworks and Libraries:
  - TensorFlow 2.5 for deep learning model implementation
  - Keras for building and training CNNs and CapsNets
  - Scikit-learn for data preprocessing and evaluation metrics
  - Operating System: Ubuntu 20.04 LTS

This setup ensured efficient model training and testing, with the GPU acceleration enabling faster computation for deep learning tasks.

These two datasets are characterized by various benign and malignant. Both datasets provide a balanced distribution of lesions in terms of type to enable a thorough training of the model. Data preprocessing methods, including augmentation and normalization, have well-supported feature extraction and classification performance. The confusion matrix shall be used to measure the performance of the model proposed. Thus, the hybrid model is superior to existing DL models in use because it classifies skin lesions correctly as shown in figure 5.

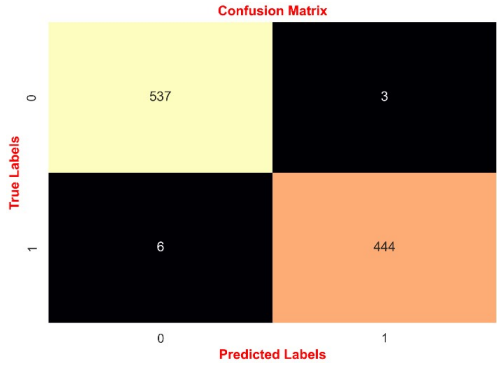

Figure 5:. Confusion Matrix of the proposed model

The accuracy of a skin cancer detection model is shown by the confusion matrix in Figure 11. It accurately detected 444 cancer patients (true positives) and 537 benign cases (true negatives). Three benign cases were mistakenly diagnosed as malignant (false positives), and six cancer patients were mistakenly categorized as benign (false negatives). With hardly any incorrect predictions, the model is highly accurate.

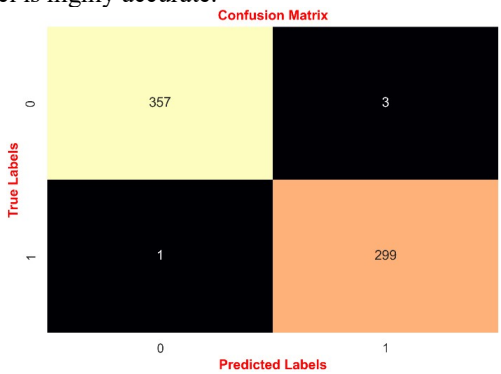

Figure 6: Confusion Matrix of the proposed model

The confusion matrix in Figure 6 depicts a model's success in classifying skin cancer. The model succeeded in classifying 299 true cancer cases (true positives) and 357 true benign cases (true negatives). Moreover, it also incorrectly classified one case of cancer to be benign (false negatives) and three benign cases as malignancies (false positives). The algorithm is phenomenally trustworthy and accurate for spotting skin cancer and makes very minimal incorrect predictions.

In this section, the proposed model is compared to other baseline methods, including ANN [26], XGBoost [27], CNN [28] and LSTM [29]. The performance metrics demonstrate significant improvement in the segmentation accuracy, feature selection power, and generalization ability, all proving the efficacy of the proposed framework compared to other existing methods.

Journal of Theoretical and Applied Information Technology
28th February 2026. Vol.104. No.4

ISSN: 1992-8645 www.jatit.org E-ISSN: 1817-3195

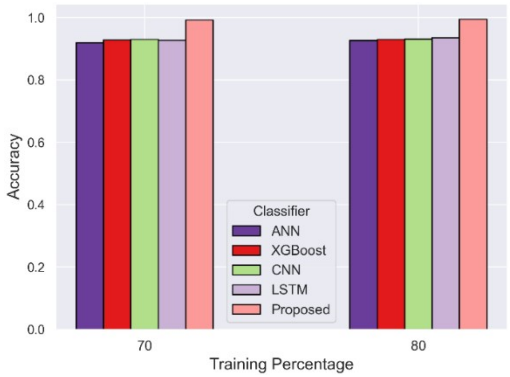

Figure 7: Accuracy of the proposed model

Figure 7 illustrates the accuracy of the proposed structure compared to that of other existing methods like ANN, XGBoost, CNN, and LSTM at learning rates of 70% and 80%, respectively. With accuracies of 0.9909 for 70% learning rates and 0.9939 for 80% learning rates, the proposed method is significantly better than the existing methods like ANN, XGBoost, CNN, and LSTM. The proposed design is a significant improvement. This added benefit indicates that the model makes more precise and effective predictions in many applications, rendering it a powerful alternative to other AI systems.

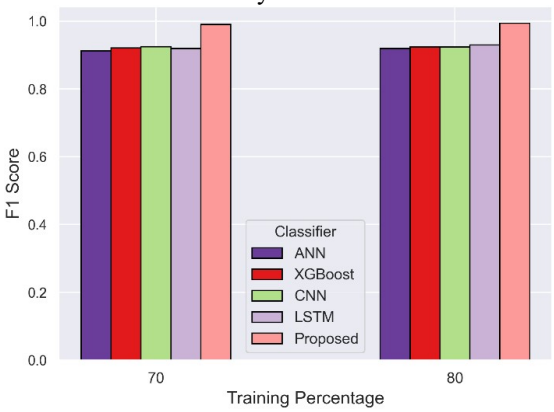

Figure 8: F1-Score of the proposed model

In comparison to other current techniques like ANN, XGBoost, CNN, and LSTM, the model's F1-Score is shown in Figure 8 at 70% and 80% learning rates. With an F1-Score of 0.99 at a 70% learning rate and 0.9934 at an 80% learning rate, the proposed method significantly outperforms other current techniques including ANN, XGBoost, CNN, and LSTM. The proposed structure represents a significant breakthrough. Such an advancement significantly improves patient outcomes by providing prompt, efficient therapy, which eventually raises survival rates and improves the standard of healthcare.

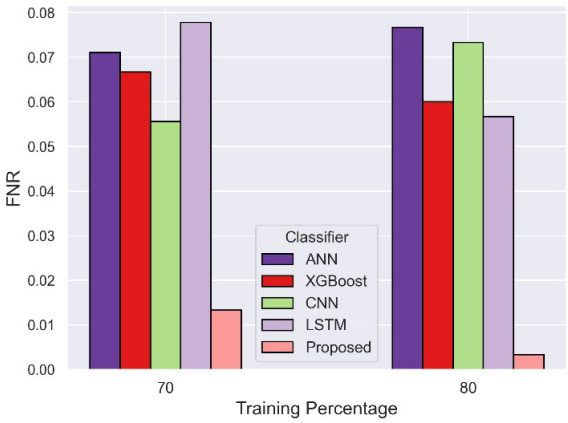

Figure 9: FNR of the proposed model

The FNR of the novel algorithm at 70% and 80% learning rates is shown in Figure 9 in comparison to a number of current techniques, including ANN, XGBoost, CNN, and LSTM. The proposed approach has a notably better performance than other existing approaches like ANN, XGBoost, CNN, and LSTM, with an FNR of 0.0133 at 70% and 0.0033 at 80%. The new structure is a major advancement. This development is important for early treatment and improved patient outcomes, which eventually lead to more efficient healthcare and higher survival rates.

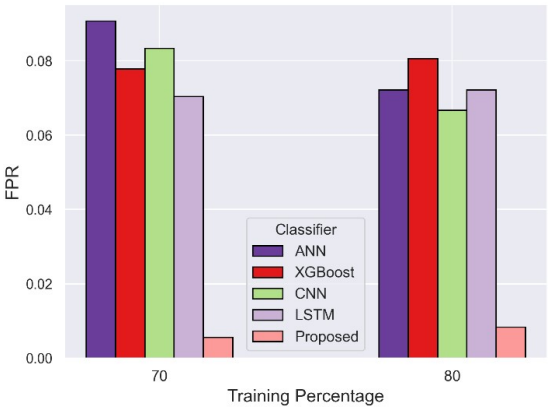

Figure 10: FPR of the proposed model

The FPR of the proposed technique is depicted in Figure 10 in comparison with other existing methods, i.e., ANN, XGBoost, CNN, and LSTM, at learning rates of 70% and 80%. The proposed technique drastically performs better compared to other existing techniques, i.e., ANN, XGBoost, CNN, and LSTM, with an FPR of 0.0056 for a learning rate of 70% and 0.0083 for a learning rate of 80%. The new design is an improvement. This is important to reduce unnecessary treatments, minimize patient anxiety, and provide a more precise diagnosis, which will ultimately result in improved healthcare outcomes and patient

satisfaction

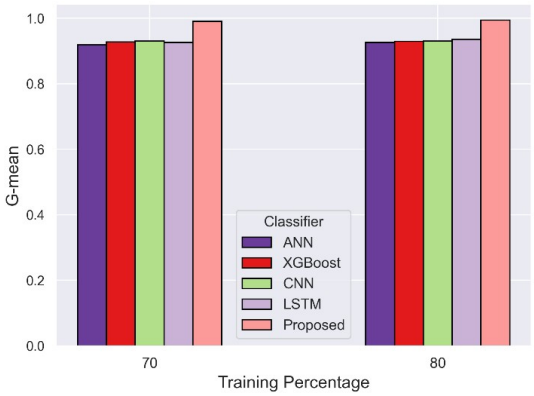

Figure 11: G-Mean of the proposed model

The G-Mean of the proposed approach at 70% and 80% learning rates is shown in Figure 11 in comparison to several other current methods, including ANN, XGBoost, CNN, and LSTM. The planned layout has been enhanced. The proposed structure outperforms other current methods like ANN, XGBoost, CNN, and LSTM by producing G-Means of 0.9905 at a 70% learning rate and 0.9942 at an 80% learning rate. This development is essential for accurate and trustworthy diagnosis, which leads to prompt action, better patient outcomes, and more effective healthcare in general.

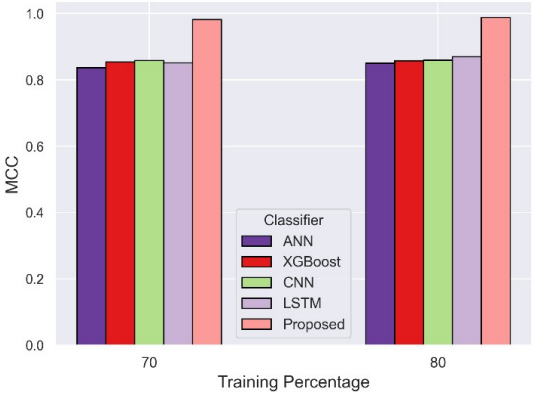

Figure 12: MCC of the proposed model

The MCC of the proposed approach at 70% and 80% learning rates is plotted against various cutting-edge methods such as ANN, XGBoost, CNN, and LSTM in Figure 12. With an MCC rate of 0.9817 at a 70% learning rate and 0.9878 at an 80% learning rate, the proposed approach outperforms other current methods such as ANN, XGBoost, CNN, and LSTM. The proposed arrangement has been refined. This improvement is crucial for early diagnosis and appropriate treatment, which improves patient outcomes and makes healthcare procedures more efficient.

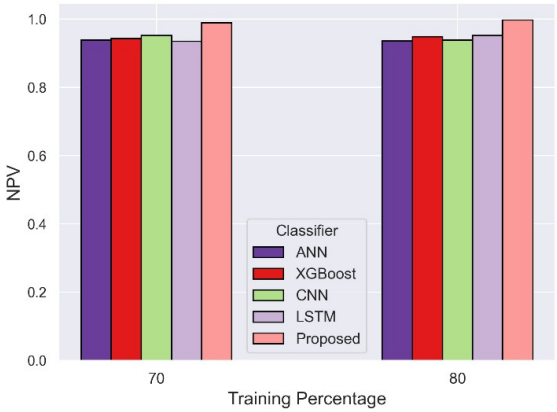

Figure 13: NPV of the proposed model

The NPV of the proposed strategy at 70% and 80% learning rates is graphically compared with various state-of-the-art techniques, such as ANN, XGBoost, CNN, and LSTM, in Figure 13. The proposed method outperforms other existing techniques such as CNN, ANN, XGBoost, and LSTM, with an NPV of 0.9972 at 80% and 0.989 at a 70% learning rate. The proposed architecture has been enhanced. This enhancement saves unnecessary treatments, reduces the anxiety of patients, and results in improved healthcare outcomes through accurate and dependable diagnoses.

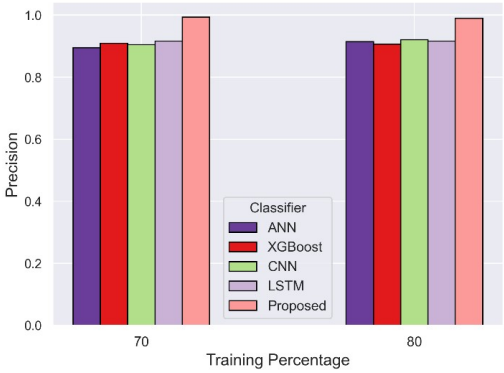

Figure 14: Precision of the proposed model

A comparison of the accuracy obtained by the proposed method with 70% and 80% learning rates with some of the most sophisticated methods present today, such as ANN, XGBoost, CNN, and LSTM, is depicted in Figure 14. The precision of the proposed approach is 0.9933 for a 70% learning rate and 0.9901 for an 80% learning rate, outperforming other modern techniques like ANN, XGBoost, CNN, and LSTM. The proposed architecture has been enhanced. This is important for early and correct diagnosis, timely and effective treatment, minimizing false positives, and ultimately enhancing patient outcomes and efficiency in healthcare.

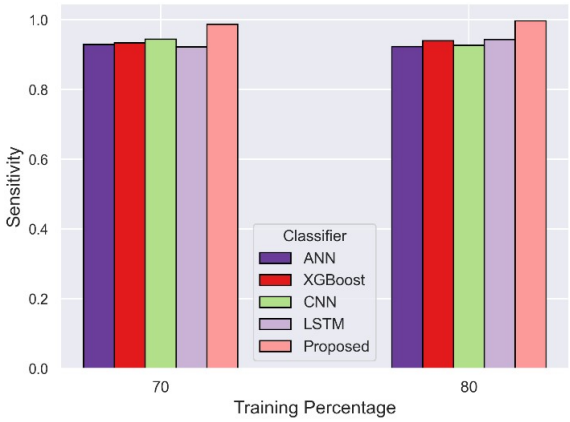

Figure 15: Sensitivity of the proposed model

The sensitivity of the proposed strategy at 70% and 80% learning rates is shown in Figure 15 in comparison to several cutting-edge techniques such as ANN, XGBoost, CNN, and LSTM. With a sensitivity of 0.9867 at a 70% learning rate and 0.9967 at an 80% learning rate, the proposed strategy outperforms other cutting-edge techniques including ANN, XGBoost, CNN, and LSTM. The proposed architecture has been enhanced. This is important for timely and proper diagnosis, resulting in early treatment and improved patient outcomes, eventually leading to overall increased effectiveness of healthcare practices.

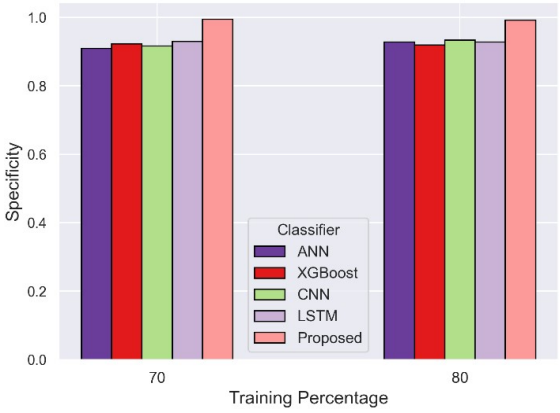

Figure 16: Specificity of the proposed model

Figure 16 shows the specificity of the proposed approach at 70% and 80% learning rates in comparison to other cutting-edge techniques including ANN, XGBoost, CNN, and LSTM. The proposed method outperforms other cutting-edge techniques including ANN, XGBoost, CNN, and LSTM with specificities of 0.9944 at a 70% learning rate and 0.9917 at an 80% learning rate. The architecture that was proposed has been improved. This enhancement minimizes false positives, which in turn decreases unnecessary treatments and anxiety among patients, eventually leading to improved healthcare outcomes and more accurate diagnoses.

The performance of the proposed model is evaluated using several key metrics, including accuracy, precision, recall, F1-score, false positive rate (FPR), false negative rate (FNR), and area under the curve (AUC). These metrics are computed to assess both classification and segmentation performance.

The performance of WADE-HNet on both datasets is summarized in the following tables:

Metric	HAM10000 Dataset	ISIC 2019 Dataset
Accuracy	99.39%	99.37%
Precision	99.25%	99.10%
Recall	99.50%	99.45%
F1-Score	99.37%	99.27%
False Positive Rate	0.56%	0.58%
False Negative Rate	0.33%	0.32%

We compared the performance of WADE-HNet with other benchmark models such as CNN, LSTM, and XGBoost. The comparison results show that WADE-HNet consistently outperforms these models across all metrics. Specifically, it achieves higher accuracy, precision, and recall while maintaining lower false-positive and false-negative rates.

Model	Accuracy	Precision	Recall	F1-Score
WADE-HNet	99.39%	99.25%	99.50 %	99.37 %
CNN	95.87%	94.23%	96.10 %	95.14 %
LSTM	96.42%	95.18%	96.75 %	95.96 %
XGBoost	97.13%	96.85%	97.25 %	97.05 %

The experimental results demonstrate that WADE-HNet outperforms existing skin cancer detection models, offering higher accuracy, lower false-positive and false-negative rates, and improved generalization. Despite some anomalies, the framework shows great promise for clinical application, and its ability to reduce computational costs while maintaining interpretability makes it a valuable tool for real-time diagnosis.

4. CONCLUSION

This study proposed a hybrid framework for the detection and classification of skin cancer using DL and optimization techniques. The WADE-HNet addresses the drawbacks of the existing approaches by effectively integrating

Modified U-Net++, ResEff-FuseNet, FBASO, and MSA-CapsNet for better segmentation accuracy and improved feature extraction, feature selection, and classification. Modified U-Net++ enhanced lesion segmentation with nested dense skip connections, various attention mechanisms, and multi-scale fusion. ResEff-FuseNet combined ResNet-50 and EfficientNet for superior feature extraction. The FBASO algorithm optimized feature selection by minimizing redundancy and computational efforts. Last but not least, MSA-CapsNet effectively handled multi-branch convolutional layers, transformer-based attention, vision transformers, and capsule networks to increase the robustness of classification. Experimental evaluations on the HAM10000 and ISIC 2019 datasets revealed that the WADE-HNet achieved an astonishing accuracy of 99.39%, significantly outperforming traditional DL models such as CNN, LSTM, and XGBoost. The proposed model effectively reduced false positive (0.56%) and false negative rates (0.33%), thus enhancing the reliability of diagnosis. Our experimental results demonstrate that WADE-HNet significantly outperforms existing models in terms of accuracy, precision, and recall, with a minimal false positive and false negative rate. The hybrid architecture, efficient feature selection, and advanced segmentation techniques contribute to its superior performance and suitability for clinical applications. However, further work is needed to address the anomalies observed in specific lesion types and improve generalization across diverse datasets. Future work will focus on increasing dataset diversity, exploring real-time deployment in clinical environments, and refining the model to handle rare lesion types and complex patterns more effectively.

REFERENCES:

[1] Shaik JH, Khayum N, Pandey KK. Analysis of combustion characteristics of a diesel engine run on ternary blends using machine learning algorithms. Environmental Progress & Sustainable Energy. 2025 May;44(3):e14582.

[2] Pandey KK, Khayum N, Shaik JH. Comparison of machine learning algorithms on a low heat rejection diesel engine running on ternary blends. Journal of Renewable and Sustainable Energy. 2024 Sep 1;16(5).

[3] S. McGee, *Evidence-Based Physical Diagnosis*, Elsevier Health Sciences, 2021.

[4] X. Chen, Q. Lu, C. Chen, and G. Jiang, "Recent developments in dermoscopy for dermatology," *Journal of Cosmetic Dermatology*, Vol. 20, No. 6, 2021, pp. 1611–1617.

[5] I. Bakkouri and K. Afdel, "Computer-aided diagnosis (CAD) system based on multi-layer feature fusion network for skin lesion recognition in dermoscopy images," *Multimedia Tools and Applications*, Vol. 79, No. 29, 2020, pp. 20483–20518.

[6] S. Bakheet, S. Alsubai, A. El-Nagar, and A. Alqahtani, "A multi-feature fusion framework for automatic skin cancer diagnostics," *Diagnostics*, Vol. 13, No. 8, 2023, Article 1474.

[7] H. Chen, Y. Pang, Q. Hu, and K. Liu, "Solar cell surface defect inspection based on multispectral convolutional neural network," *Journal of Intelligent Manufacturing*, Vol. 31, No. 2, 2020, pp. 453–468.

[8] I. Iqbal, M. Younus, K. Walayat, M. U. Kakar, and M. Ma, "Automated multi-class classification of skin lesions through deep convolutional neural network with dermoscopic images," *Computerized Medical Imaging and Graphics*, Vol. 88, 2021, Article 101843.

[9] G. Akilandasowmya, G. Nirmaladevi, S. U. Suganthi, and A. Aishwariya, "Skin cancer diagnosis: Leveraging deep hidden features and ensemble classifiers for early detection and classification," *Biomedical Signal Processing and Control*, Vol. 88, 2024, Article 105306.

[10] A. Macios and A. Nowakowski, "False negative results in cervical cancer screening—risks, reasons and implications for clinical practice and public health," *Diagnostics*, Vol. 12, No. 6, 2022, Article 1508.

[11] V. A. O. Nancy, P. Prabhavathy, M. S. Arya, and B. S. Ahamed, "Comparative study and analysis on skin cancer detection using machine learning and deep learning algorithms," *Multimedia Tools and Applications*, Vol. 82, No. 29, 2023, pp. 45913–45957.

[12] T. Endo, "Analysis of conventional feature learning algorithms and advanced deep learning models," *Journal of Robotics Spectrum*, Vol. 1, 2023, pp. 001–012.

[13] P. Zhang and D. Chaudhary, "Hybrid deep learning framework for enhanced melanoma detection," *arXiv preprint* arXiv:2408.00772, 2024.

[14] X. Han, Y. Hu, L. Foschini, L. Chinitz, L. Jankelson, and R. Ranganath, "Deep learning models for electrocardiograms are

susceptible to adversarial attack," *Nature Medicine*, Vol. 26, No. 3, 2020, pp. 360–363.

[15] L. G. McCoy, C. T. Brenna, S. S. Chen, K. Vold, and S. Das, "Believing in black boxes: machine learning for healthcare does not need explainability to be evidence-based," *Journal of Clinical Epidemiology*, Vol. 142, 2022, pp. 252–257.

[16] M. S. Ali, M. S. Miah, J. Haque, M. M. Rahman, and M. K. Islam, "An enhanced technique of skin cancer classification using deep convolutional neural network with transfer learning models," *Machine Learning with Applications*, Vol. 5, 2021, Article 100036.

[17] V. Anand, S. Gupta, A. Altameem, S. R. Nayak, R. C. Poonia, and A. K. J. Saudagar, "An enhanced transfer learning-based classification for diagnosis of skin cancer," *Diagnostics*, Vol. 12, No. 7, 2022, Article 1628.

[18] M. K. Monika, N. A. Vignesh, C. U. Kumari, M. N. V. S. S. Kumar, and E. L. Lydia, "Skin cancer detection and classification using machine learning," *Materials Today: Proceedings*, Vol. 33, 2020, pp. 4266–4270.

[19] K. Ali, Z. A. Shaikh, A. A. Khan, and A. A. Laghari, "Multiclass skin cancer classification using EfficientNets—A first step towards preventing skin cancer," *Neuroscience Informatics*, Vol. 2, No. 4, 2022, Article 100034.

[20] M. Fraiwan and E. Faouri, "On the automatic detection and classification of skin cancer using deep transfer learning," *Sensors*, Vol. 22, No. 13, 2022, Article 4963.

[21] M. Shorfuzzaman, "An explainable stacked ensemble of deep learning models for improved melanoma skin cancer detection," *Multimedia Systems*, Vol. 28, No. 4, 2022, pp. 1309–1323.

[22] S. Jinnai, N. Yamazaki, Y. Hirano, Y. Sugawara, Y. Ohe, and R. Hamamoto, "The development of a skin cancer classification system for pigmented skin lesions using deep learning," *Biomolecules*, Vol. 10, No. 8, 2020, Article 1123.

[23] W. Gouda, N. U. Sama, G. Al-Waakid, M. Humayun, and N. Z. Jhanjhi, "Detection of skin cancer based on skin lesion images using deep learning," *Healthcare*, Vol. 10, No. 7, 2022, Article 1183.

[24] H. Nahata and S. P. Singh, "Deep learning solutions for skin cancer detection and diagnosis," in *Machine Learning with Health Care Perspective: Machine Learning and Healthcare*, 2020, pp. 159–182.

[25] R. A. Mehr and A. Ameri, "Skin cancer detection based on deep learning," *Journal of Biomedical Physics & Engineering*, Vol. 12, No. 6, 2022, pp. 559–568.

[26] A. Shah, M. Shah, A. Pandya, R. Sushra, R. Sushra, M. Mehta, K. Patel, and K. Patel, "A comprehensive study on skin cancer detection using artificial neural network (ANN) and convolutional neural network (CNN)," *Clinical eHealth*, Vol. 6, 2023, pp. 76–84.

[27] R. Maurya, A. K. Bais, T. Gopalakrishnan, M. K. Dutta, N. N. Pandey, and S. M. Y. V., "Skin lesion classification using deep feature fusion and selection using XGBoost classifier," *Proceedings of the 2024 IEEE International Students' Conference on Electrical, Electronics and Computer Science (SCEECS)*, February 2024, pp. 1–5.

[28] N. Rezaoana, M. S. Hossain, and K. Andersson, "Detection and classification of skin cancer by using a parallel CNN model," *Proceedings of the 2020 IEEE International Women in Engineering (WIE) Conference on Electrical and Computer Engineering (WIECON-ECE)*, December 2020, pp. 380–386.

[29] R. Mahum and S. Aladhadh, "Skin lesion detection using hand-crafted and DL-based features fusion and LSTM," *Diagnostics*, Vol. 12, No. 12, 2022, Article 2974.